Annihilation of positrons trapped at the alkali-metal-covered transition-metal surface

N. G. Fazleev,* J. L. Fry, K. H. Kuttler, A. R. Koymen, and A. H. Weiss
Department of Physics, The University of Texas at Arlington, Arlington, Texas 76019-0059
(Received 7 February 1995)

Recent studies of the Cu(100) surface covered with submonolayers of Cs [A. R. Koymen *et al.*, Phys. Rev. Lett. **68**, 2378 (1992)] revealed that the normalized intensity of the positron-annihilation-induced Cu $M_{2,3}$ VV Auger signal remains nearly constant at the clean Cu(100) surface value until the Cs coverage reaches approximately 0.7 physical monolayer, at which coverage the signal intensity drops precipitously. We present a microscopic analysis of this unusual behavior of the Cu $M_{2,3}VV$ Auger signal based on a treatment of a positron as a single charged particle trapped in a "correlation well" in the proximity of the surface atoms. The image-potential-induced positron surface states are calculated using the corrugated-mirror model in a full three-dimensional geometry. These states are studied for the clean Cu(100) surface and for various ordered structures of the Cs adsorbate on the Cu(100) surface below and above the critical alkali-metal coverage of approximately 0.7 physical monolayer. Calculations show that whereas the positron surface state is localized in the region of the Cs/Cu(100) interface for Cs coverages below the critical alkali-metal coverage, at a Cs coverage corresponding to one physical monolayer the positron surface state is localized on the vacuum side of the Cs overlayer. The probabilities for a positron trapped in a surface state to annihilate with relevant Cu and Cs core-level electrons as well as the positron surface-state lifetimes are computed for various alkali-metal structures on the Cu(100) surface and compared with experimental positron-annihilation-induced Auger-electron-spectroscopy data. It is shown that a shift in localization of the positron surface state from the Cs/Cu(100) interface to the vacuum side of the alkali-metal overlayer results in a sharp decrease in the positron-annihilation probabilities with Cu $3s$ and $3p$ core-level electrons, in agreement with experiment.

I. INTRODUCTION

Alkali-metal adsorption on transition-metal surfaces has been studied extensively due to its wide variety of electronic properties which are important from both fundamental and technological points of view.[1–10] In spite of longtime experimental and theoretical efforts, there are a number of unsolved problems with regard to the alkali-metal adsorption on metal surfaces. Among them, the distinct property of chemisorbed alkali-metal adatoms to reduce significantly the electron work function of the substrate has attracted a great deal of attention because of its relevance to cathode technology. Recently alkali-metal adsorption on transition-metal surfaces has become the subject of experimental studies using the surface characterization technique, positron-annihilation-induced Auger-electron spectroscopy (PAES).[11–16] In PAES a fraction of the low-energy positrons trapped in the positron surface state annihilate with neighboring core-level electrons, creating core-hole excitations which give rise to the Auger-electron emission.[17] A unique feature of PAES is that the electrons which make up the Auger peak in the electron energy spectrum originate almost exclusively from atoms in the outermost layer of the surface.[12] As a result, PAES is more surface sensitive than standard methods of the Auger-electron excitation. In the case of the electron (or photon) excitation of core holes, the Auger electrons originate from an excitation volume which extends hundreds of atomic layers below the surface, limiting the surface selectivity to the escape depth of the Auger electron (of the order of 5–20 Å).[18] The applicability of PAES to the measurement of thermal desorption of positrons from the surface state,[19] to the compositional characterization of the topmost atomic layer, and to the study of the initial stages of epitaxial growth, interdiffusion, and alloy formation has been already established.[11,12,20–22] In addition, since PAES intensities are sensitive to the spatial distribution of the positron wave function on the surfaces of interest, the method can be applied to study the nature and location of the positron surface state.[23]

In PAES studies of the alkali-transition-metal surface, Koymen *et al.*[11] found that the normalized intensity of the positron-annihilation-induced Cu $M_{2,3}VV$ Auger signal, I_P, obtained as a function of Cs coverage on a Cu(100) surface at 163 K drops sharply in a range of less than 0.02 monolayer at a critical Cs coverage of approximately 0.70 physical monolayer [one physical monolayer of a hexagonal-close-packed array of Cs atoms on the (100) surface of copper corresponds to the highest coverage of 0.416×10^{15} atoms/cm^2 that can be accommodated in a single layer on the surface[9]]. Due to the fact that in the energy range of PAES measurements almost all holes in the core levels give rise to Auger-electron emission,[24] the experimental PAES intensities are directly related to the core-annihilation probabilities $p_{n,l}$, i.e., the fractions of positrons trapped in a surface state annihilating with electrons from different core shells with quantum numbers n and l ($n=1,2,3,\ldots;l=s,p,d,\ldots$). This implies that the sum of the annihilation probabilities of surface-trapped positrons with Cu $3s$ and $3p$ core-level electrons changes abruptly from the relatively high combined

0163-1829/95/52(7)/5351(13)/$06.00

core-annihilation probabilities to much lower combined core-annihilation probabilities when the Cs coverage reaches 0.70 physical monolayer. (The majority of 3*s* holes in the Cu core decay through the $M_1M_{2,3}V$ Auger channel, leaving a hole in the Cu 3*p* shell which results in the subsequent $M_{2,3}VV$ Auger emission.[14])

These experimental PAES results deviate significantly from predictions by Nieminen and Jensen.[25] According to their calculations of the positron surface states at the alkali-metal-covered Ni surfaces, the charge rearrangement with the alkali-metal adsorption that leads to the lowering of the electron work function causes the positron to become mainly localized in the region between the substrate and the overlayer up to an alkali-metal coverage of one physical monolayer.[25] This location of a positron bound state results in a relatively large overlap of the positron density function and the substrate core electron-density functions, and predicts that the core-annihilation probabilities are insensitive to changes in the alkali-metal coverage. Thus, according to calculations by Nieminen and Jensen,[25] the Cu $M_{2,3}VV$ PAES signal should remain close to the clean surface value after deposition of Cs up to one physical monolayer. A relatively modest reduction in the Cu $M_{2,3}VV$ PAES intensity is expected due to attenuation caused by the inelastic scattering of the outgoing Auger electrons as they traverse the Cs overlayer.

Koymen *et al.*[11] performed calculations of the Cu PAES signal intensity based on the approach of Nieminen and Jensen[25] for the ordered $p(2\times2)$ and $c(2\times2)$ arrangements of Cs adatoms on the Cu(100) surface which correspond to alkali-metal coverages of 0.49 and 0.98 physical monolayer, respectively. However, the results of those calculations are in reasonable agreement with the experimental data only below the critical Cs coverage.[11] Those calculations do not reproduce the sharp drop in the Cu PAES intensity observed for the Cs/Cu(100) system at the Cs coverage of approximately 0.70 physical monolayer, and greatly overestimate the intensity of the positron-annihilation-induced Cu $M_{2,3}VV$ Auger signal observed for Cs coverages exceeding the critical one.[11]

Fazleev and co-workers[15,16] were able to account for the observed behavior of the intensity of the Cu PAES signal with the Cs coverage in the context of a phenomenological model, which treats the positron as trapped in a double-well potential in the direction perpendicular to the surface (one well is located just outside the Cu substrate and the other is located on the vacuum side of the alkali-metal adsorbate metallic islands). The sharp drop in the Cu $M_{2,3}VV$ PAES intensity observed for the Cs/Cu(100) system at the critical alkali-metal coverage of approximately 0.70 physical monolayer was attributed to a shift of positrons trapped at low Cs coverages in the bound state at the Cs/Cu interface to the positron surface state on the vacuum side of the Cs overlayer at high alkali-metal coverages. The appearance of the positron surface state on the vacuum side of the Cs overlayer over a small change in the Cs coverage at the critical alkali-metal coverage was assumed to be due to a structural phase transition in the Cs overlayer from a disordered distribution of adatoms to adsorbate metallic islands with an ordered hexagonal-close-packed structure.

The purpose of this paper is to present an *ab initio* analysis of the results of PAES studies of the alkali-transition surface by performing first-principles calculations of the positron surface state and corresponding positron-annihilation characteristics for the Cu(100) surface covered with submonolayers of Cs. Such calculations are indispensable in order to clarify the Cs coverage dependence of the normalized Cu $M_{2,3}VV$ PAES intensity and the localization of the positron bound state at the alkali-transition-metal surface. In Sec. II we perform calculations of positron surface states for the clean Cu(100) surface and for various ordered structures of the Cs adsorbate on the Cu(100) surface below and above the critical alkali-metal coverage of 0.7 physical monolayer. In Sec. III positron-annihilation characteristics are determined. The impact of various arrangements of the Cs adsorbate on annihilation probabilities of surface-trapped positrons with copper 3*s* and 3*p* core-level electrons as well as with cesium 4*p* and 4*d* core-level electrons is discussed, and positron surface-state lifetimes are calculated. In Sec. IV we compare our calculations of the annihilation probabilities of a positron trapped in surface states with relevant Cu and Cs core-level electrons for various ordered structures of the Cs adsorbate on the Cu(100) surface below and above the critical alkali-metal coverage with experimental measurements of the PAES intensities as a function of Cs coverage performed at low temperatures. Conclusions are made in Sec. V.

II. POSITRON SURFACE STATES

Calculations of the positron surface state in the present paper are performed using the corrugated-mirror model of Nieminen and Puska.[26] Within this model the trapping of the positron in a correlation well in the proximity of surface atoms is calculated on the basis of a long-range (nonlocal) image potential which is made to have the same corrugations as the total electron density at a surface. Earlier calculations based on this model have been successful in analyzing the appearance and stability of positron surface states at transition-metal surfaces.[14,25,26] The potential due to the surface felt by a positron may be written as

$$V(\mathbf{r})=V_H(\mathbf{r})+V_{\rm corr}(\mathbf{r}) , \tag{1}$$

where $V_H(\mathbf{r})$ is an electrostatic Hartree part, and $V_{\rm corr}(\mathbf{r})$ is a correlation component of the positron potential. The two terms of this potential will be discussed separately below.

A. Hartree potential for a positron at a metal surface

The Hartree potential $V_H(\mathbf{r})$ is constructed as a superposition of the atomic Coulomb potentials from all the atoms located within a predetermined radius of the evaluation point. Atomic calculations for each atomic species are performed within the local-spin-density approxima-

tion,[27] using the exchange-correlation functional and atomic configurations from Refs. 28 and 29, respectively. The termination of the bulk metal at the surface results in a charge imbalance at the surface and in the presence of the surface dipole layer that is not compensated for by an additional layer of metal. This charge imbalance at the surface is a source of a net dipole term on the surface which effects the electron distribution functions on the surface, and results in the surface dipole term in the positron potential. As a result, the calculated positron ground-state energy E_∞ for the bulk differs by ΔD_0 from the measured positron work function Φ_+.[14,25] An additional contribution ΔD to the surface dipole term is due to alkali-metal adsorbates. This latter term is dependent on the alkali-metal coverage of the transition-metal surface, the type of adsorbate, and the type of substrate metal. To correct for misrepresentation of the surface dipole in the atomistic-superposition model, a ramp potential[14,25] can be added to the expression for the total positron potential. The height $\Delta V = -\Phi_+ - E_\infty$ is adjusted for each surface to give the correct positron work function. However, in the calculations presented in this paper the surface dipole layer effects on the electron distribution functions at the surface and on the positron potential are taken into consideration using the method of Weinert and Watson.[30] This method avoids the introduction of arbitrary parameters associated with the use of the ramp potential,[14,25] as well as difficulties associated with the positioning of the ramp potential at arbitrary alkali-metal coverages. Following the method of Weinert and Watson[30] the atoms are placed in a compensating potential well of magnitude -0.25 Ry extending from the atom center out to one Wigner-Seitz radius, then linearly ramping to a value of 0.00 Ry at twice the Wigner-Seitz radius and beyond. (The Wigner-Seitz radius is defined as the radius of a sphere with the same volume as the polyhedron Wigner-Seitz unit cell.) This potential well has been used for a large variety of metal surfaces and produces results for the electron work function in reasonable agreement with the experimental data.[30] The Schrödinger equation is solved self-consistently for each bound electron state of each atomic species initially using the Thomas-Fermi potential for the atomic potential with the inclusion of the compensating potential well. Then with the resulting atomic charge density, Poisson's equation is used with a small screening function[31] to derive a potential estimate. An atomic potential is found by mixing the result of Poisson's equation with the initial potential estimate and adding the compensating potential well to force the inclusion of the surface dipole effect. Then the Schrödinger equation is solved using the potential, and the calculations are repeated until the process converges. Coulomb potentials for each atomic species at the surface are finally constructed from Poisson's equation using the three-dimensional atomic charge densities derived through self-consistent iteration. The crystal structure and the lattice constant for copper are taken from Ref. 29. It has been verified that the resulting total electron charge densities for each atomic species agree with the self-consistent potential expected on the surface of a solid.[30]

B. Correlation potential for a positron at a metal surface

The correlation component $V_{\text{corr}}(\mathbf{r})$ of the positron potential in regions of high electron density is constructed using a local-density approximation. In these regions $V_{\text{corr}}(\mathbf{r})$ becomes a function of the total three-dimensional electron density, $n(\mathbf{r})$, described by a superposition of atomic electron densities.[32] The parametrization by Boronski and Nieminen[33] is used for the electron-density dependence of $V_{\text{corr}}(\mathbf{r})$. Following the corrugated mirror model,[26] the correlation part of the total positron potential outside the metal surface is expressed as an image potential,

$$V_{\text{image}}(\mathbf{r}) = -\frac{e^2}{4\pi\varepsilon_0}\frac{1}{4[Z_{\text{eff}}(n(\mathbf{r})) - Z_0]}\ , \tag{2}$$

where e is the charge of a positron, ε_0 is the vacuum permittivity, $Z_{\text{eff}}(n(\mathbf{r}))$ is the effective distance from the surface, represented as a function of the total electron density at the surface, $n(\mathbf{r})$, and Z_0 defines the effective image-plane position on the vacuum side of the top layer of atoms. The image potential is constructed to have the same corrugations, i.e., the same constant-value surfaces, as the total electron density $n(\mathbf{r})$. The effective distance $Z_{\text{eff}}(n(\mathbf{r}))$ in the denominator of Eq. (2) is determined by inverting the function $n(Z_{\text{eff}})$ along a reference line normal to the surface from a center of the adsorbate atom on the Cu(100) surface, or from a center of the reference atom on the Cu substrate (100) surface if no adsorbate is present. The assumption is made that at large distances (low electron density) the corrugations in the image potential are negligible, and that Z_{eff} is equal to the coordinate perpendicular to the surface. The joining of the image potential to the local-density correlation potential is done by taking V_{corr} to be the larger of the two at each point outside the surface.

Since the compensating potential well introduced in our atomic calculations accounts for the surface dipole effects, there is no need for the additional introduction of a ramp potential to the expression for the total positron potential: E_∞ now becomes equal to $-\Phi_+$, thus giving a zero value for the ramp potential ΔV.

C. Positrons at the Cu(100) surface

The positron is assumed to be in the ground state in the image correlation well at the surface, and is delocalized in the plane of the surface. The positron potential is defined on the three-dimensional mesh with an initial mesh spacing of 1.705 atomic units. The numerical solution of the Schrödinger equation is obtained using a modified relaxation technique.[26] The positron binding energy and the positron wave function are found by iteratively solving for the energy, and then correcting the wave function based on the energy, the positron potential, and the surrounding values of the wave function. In numerical calculations of the positron binding energy the mesh density is doubled repeatedly until the calculated energy converges. The criteria for convergence is that the resulting energy is within 10^{-8} Hartree of the previ-

ous energy or that it is greater than the energy in the previous iteration. The computer code used in calculations is characterized by the following: (a) the atomic positions are supplied as input to the code; (b) the boundaries of the calculation cell are input by the user; and (c) the boundary conditions are periodic instead of symmetry related.

Initially calculations of the positron wave function and positron binding energy are performed for the clean Cu(100) surface. Calculations are performed using input data largely taken from Ref. 14. The outermost plane of substrate atoms is taken to reside at $Z=0$. The parameter Z_0 is chosen to be one Wigner-Seitz radius of Cu from the top layer of atoms along a reference line. The computed positron binding energy E_b converges to 2.87 eV compared to the experimental value of 2.77 eV.[23] Plots of the positron potential and the ground-state positron wave function are presented in Figs. 1 and 2. It follows from these plots that the positron is trapped in the image-correlation well just outside the clean Cu(100) surface. The ground-state positron wave function is delocalized in the surface plane, has its maximum about 3.07 a.u. outside the topmost layer of atoms, and experiences a rapid drop with distance into the Cu lattice.

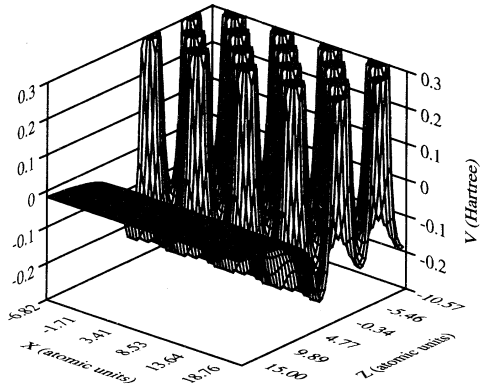

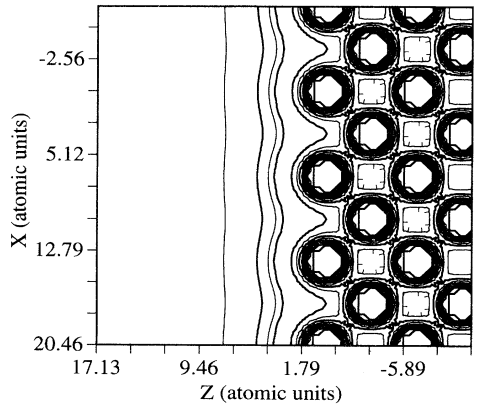

FIG. 1. Calculated potential for a positron trapped in a surface state at a clean Cu(100) surface. The upper panel shows the 3D plot. The lower panel shows the contour plot in the X-Z plane for $Y=0$. The vacuum is at the left in the lower panel. Contours are separated by 0.05 Hartree.

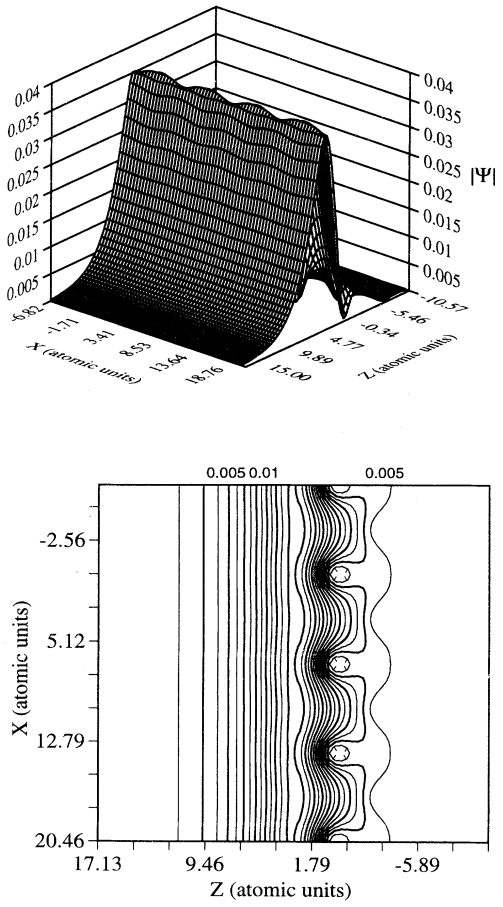

FIG. 2. Calculated ground-state wave function for a positron trapped in a surface state at a clean Cu(100) surface. The upper panel shows the 3D plot. The lower panel shows the contour plot in the X-Z plane for $Y=0$. The vacuum is at the left in the lower panel. The minimum contour and the contour spacing are 0.0025 a.u.

D. Positrons at the Cu(100) surface with submonolayers of Cs below the critical coverage

Computer simulations[16,34] of a distribution of Cs atoms [produced by randomly depositing the adatoms on the (100) surface of Cu and then allowing them to move on the two-dimensional surface due to the forces from the other adatoms and from the Cu substrate until Cs adatoms form a configuration corresponding to the lowest potential energy] show that below the coverage of 0.6 physical monolayer, Cs atoms deposited on the Cu(100) surface are distributed uniformly so that the standard deviation of the average distance between nearest neighbors is small and there are no areas with a close-packed arrangement of Cs atoms. The results of computer simulations are consistent with studies of the spectrum of col-

lective and single-particle excitations of the Cs/Cu system using electron-energy-loss spectroscopy (EELS),[6] and are supported by studies of the deposition of Cs on the Cu(100) surface by low-energy electron diffraction (LEED),[9,10] which revealed that at low temperatures (below 160 K) Cs adatoms occupy hollow sites with fourfold symmetry for coverages up to 0.7 physical monolayer. The cases of the Cs coverage below the critical coverage are modeled by positioning the Cs adsorbate on the (100) surface of Cu in the ordered $p(4\times4)$, $c(4\times4)$, and $p(2\times2)$ structures. These three arrangements result in adsorbate coverages of 0.124, 0.248, and 0.496 physical monolayers, respectively, using the Cs radius of 5.16 a.u. The adsorbate position is taken to correspond to the experimental LEED value for Cs on the Ni(100) surface: $Z_{C_s}=7.18$ a.u.[35] The image position Z_0 in the [100] direction is taken to be 3.97 a.u. outside the adsorbate layer. This value corresponds to the one obtained from the jellium calculations.[36] Plots of the positron potential and of the ground-state positron wave function for these arrangements of the Cs adsorbate on the Cu(100) surface are presented in Figs. 3–8. As it follows from calculations performed for $p(4\times4)$, $c(4\times4)$, and $p(2\times2)$ structures of the Cs adsorbate on the Cu(100) surface, the positron potential contains corrugations extending through the adsorbate overlayer into the region between the cesium atoms and the copper atoms. These corrugations form the potential well and correspond to the maximum of the positron wave function. Thus for adsorbate coverages of 0.124, 0.248, and 0.496 physical monolayers, the positron is localized mainly in the region between the Cu substrate and the Cs overlayer and not just outside the surface as in the case of the clean Cu(100) surface. The computed positron binding energies E_b with respect to vacuum for the $p(4\times4)$, $c(4\times4)$, and $p(2\times2)$ structures of the Cs adsorbate on the Cu(100) surface are equal to 3.16, 3.28, and 3.60 eV, respectively. Thus the positron binding energy E_b increases with the alkali-metal coverage relative to its value of 2.87 eV for the clean Cu sur-

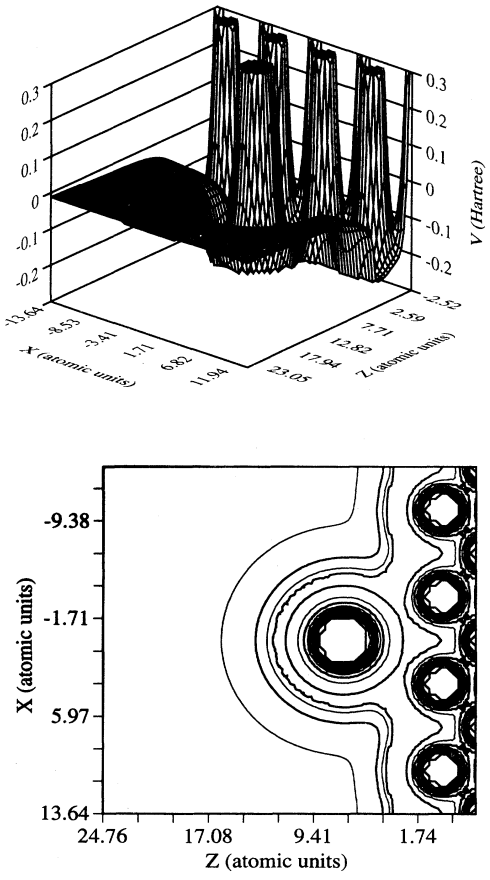

FIG. 3. Calculated potential for a positron trapped in a surface state at a Cu(100) surface with an ordered $p(4\times4)$ arrangement of the Cs adsorbate. The upper panel shows the 3D plot. The lower panel shows the contour plot in the X-Z plane for $Y=0$. The vacuum is at the left in the lower panel. Contours are separated by 0.05 Hartree.

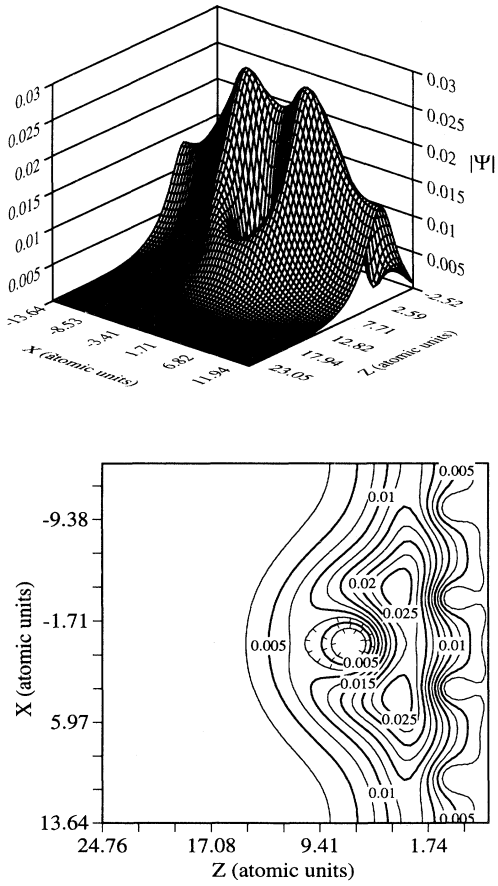

FIG. 4. Calculated ground-state wave function for a positron trapped in a surface state at a Cu(100) surface with an ordered $p(4\times4)$ arrangement of the Cs adsorbate. The upper panel shows the 3D plot. The lower panel shows the contour plot in the X-Z plane for $Y=0$. The vacuum is at the left in the lower panel. The minimum contour and the contour spacing are 0.0025 a.u.

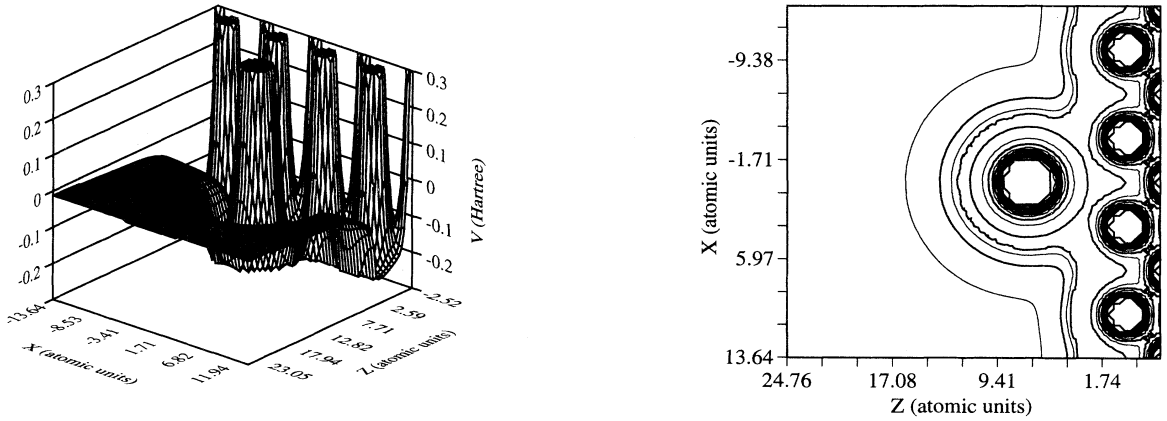

FIG. 5. Calculated potential for a positron trapped in a surface state at a Cu(100) surface with an ordered $c(4\times4)$ arrangement of the Cs adsorbate. The left panel shows the 3D plot. The right panel shows the contour plot in the X-Z plane for $Y=0$. The vacuum is at the left in the lower panel. Contours are separated by 0.05 Hartree.

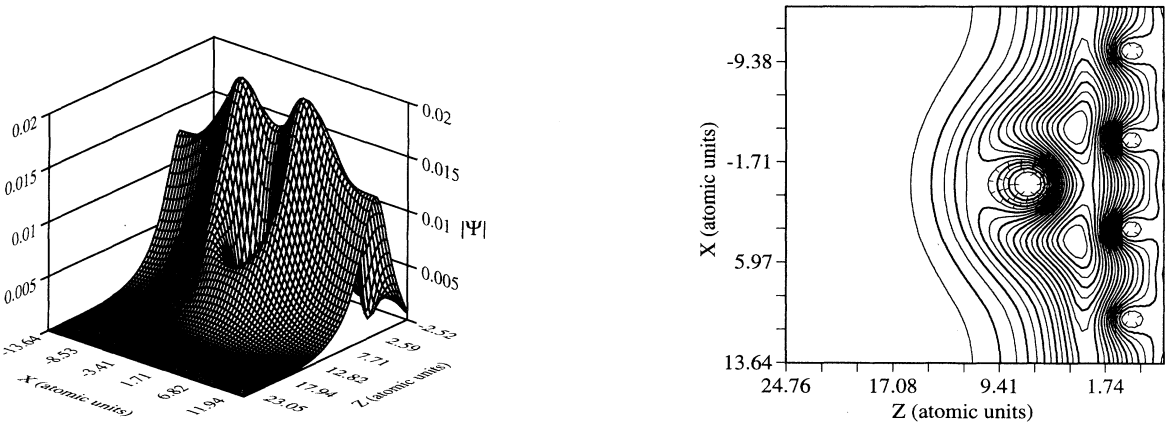

FIG. 6. Calculated ground-state wave function for a positron trapped in a surface state at a Cu(100) surface with an ordered $c(4\times4)$ arrangement of the Cs adsorbate. The left panel shows the 3D plot. The right panel shows the contour plot in the X-Z plane for $Y=0$. The vacuum is at the left in the lower panel. The minimum contour and the contour spacing are 0.001 a.u.

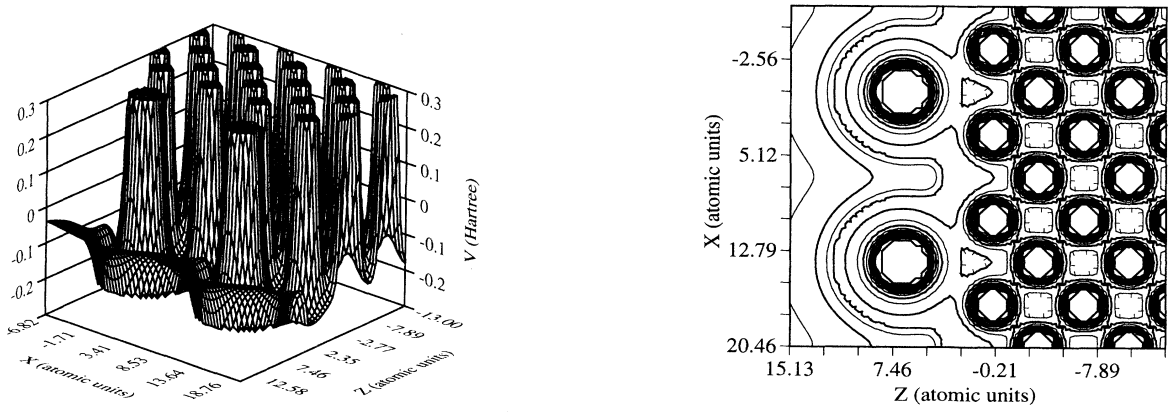

FIG. 7. Calculated potential for a positron trapped in a surface state at a Cu(100) surface with an ordered $p(2\times2)$ arrangement of the Cs adsorbate. The left panel shows the 3D plot. The right panel shows the contour plot in the X-Z plane for $Y=0$. The vacuum is at the left in the right panel. Contours are separated by 0.05 Hartree.

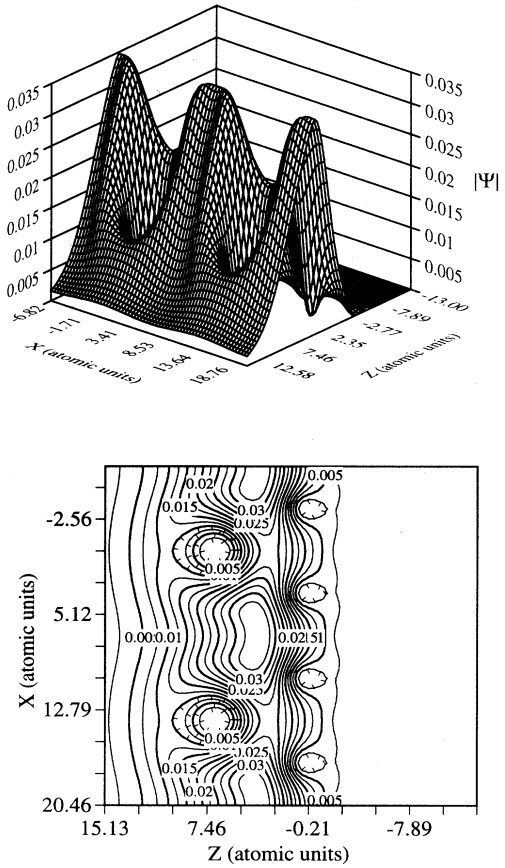

FIG. 8. Calculated ground-state wave function for a positron trapped in a surface state at a Cu(100) surface with an ordered $p(2\times2)$ arrangement of the Cs adsorbate. The upper panel shows the 3D plot. The lower panel shows the contour plot in the X-Z plane for $Y=0$. The vacuum is at the left in the lower panel. The minimum contour and the contour spacing are 0.0025 a.u.

face. This increase is consistent with the observation that the positronium thermal activation energy does not decrease as fast as the electron work function with increasing the Cs coverage.[11,16,23]

E. Positrons at the Cu(100) surface with submonolayers of Cs above the critical coverage

Computer simulations of the distribution of Cs atoms randomly deposited on the (100) surface of copper, discussed previously in Refs. 16 and 34, show that Cs adatoms start clustering at coverages of approximately 0.6 physical monolayer, and from the coverage of approximately 0.7 physical monolayer alkali-metal adatoms start to form adsorbate islands increasing in area with a locally ordered hexagonal-close-packed structure. Thus at a critical Cs coverage of approximately 0.7 physical monolayer the Cs adsorbate in the Cs/Cu(100) system experiences a structural phase transition from a disordered distribution of adatoms to adsorbate islands with a locally ordered hexagonal-close-packed structure. At an alkali-metal coverage of one physical monolayer the Cs overlayer on the Cu(100) surface has an ordered hexagonal-close-packed structure. These results are consistent with LEED observations.[9,10] The variation of the electron work function with the Cs coverage of the transition-metal surfaces suggests that the Cs overlayer is essentially neutral at coverages close to a full monolayer[2-4] (when Cs atoms are arranged in an ordered hexagonal-close-packed structure). Calculations performed within the framework of the local-density-functional theory of the magnitude of the charge between neighboring alkali-metal atoms indicate that the Cs overlayer has a metallic character at coverages close to a full monolayer.[5] Similar results with respect to the properties of alkali-metal overlayers on transition-metal surfaces are obtained in experimental investigations by Lindgren and Wallden[6] and Riffe and co-workers.[8] Thus, as the Cs coverage reaches the value of approximately 0.7 physical monolayer, the areas with an ordered hexagonal-close-packed structure

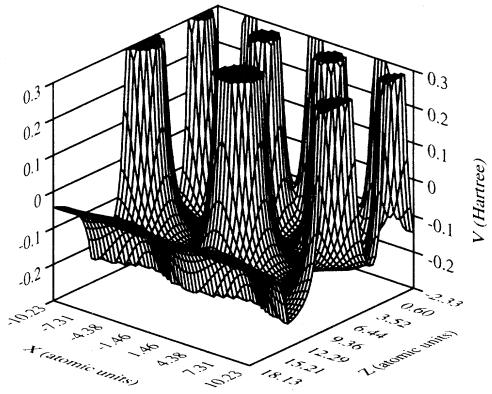

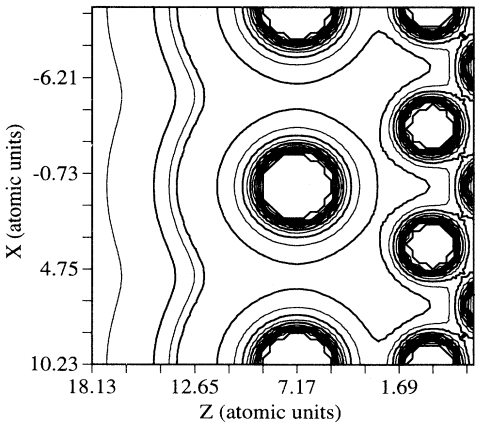

FIG. 9. Calculated potential for a positron trapped in a surface state at a Cu(100) surface with an ordered hexagonal-close-packed arrangement of the Cs adsorbate. The upper panel shows the 3D plot. The lower panel shows the contour plot in the X-Z plane for $Y=0$. The vacuum is at the left in the lower panel. Contours are separated by 0.05 Hartree.

of Cs atoms appear in the alkali-metal overlayer, signaling the onset of a structural phase transition. In these ordered hexagonal-close-packed areas, Cs atoms lose their atomic character and form the metallic adsorbate.

The case of the Cs coverage above the critical coverage is modeled by the Cs adsorbate on the Cu(100) surface in an ordered hexagonal-close-packed arrangement. This arrangement of Cs adatoms, which correspond to the Cs coverage of one physical monolayer, is not commensurate with the Cu lattice due to the larger size of the Cs atom. This noncommensurate lattice structure eliminates the symmetry of the previously calculated ordered structures of Cs on the (100) surface of Cu. The position of the image surface Z_0 from the top layer of Cs atoms along a reference line is chosen to be the Cs radius of 5.16 a.u. due to the metallic character of the Cs adsorbate at the coverage of one physical monolayer. Plots of the positron potential and the positron wave function are presented in Figs. 9 and 10. The positron potential for this Cs coverage contains small corrugations that do not extend into the substrate, but only exist on the vacuum side of the Cs overlayer. Instead of being trapped in the region between the Cs adsorbate and the Cu substrate, the positron now [similar to the case of the clean Cu(100) surface] is mainly localized on the vacuum side of the Cs overlayer. The ground-state positron wave function has its maximum about 2.91 a.u. outside the alkali-metal adsorbate, and experiences a rapid drop with distance into the Cu lattice with the Cs adsorbate. The other important result is that the calculated positron binding energy E_b for the Cs coverage of one physical monolayer is equal to 4.37 eV and is substantially larger than that for the clean Cu(100) surface. Thus the alkali-metal adsorption leads to an increase in the positron binding energy via a mechanism where at Cs coverages below the critical coverage the positron becomes localized mainly in the region between the Cu substrate and the Cs overlayer, and at alkali-metal coverages exceeding the critical coverage the positron becomes localized mainly on the vacuum side of the Cs overlayer. The increase in the positron binding energy together with the decrease of the electron work function for Cs/Cu(100) (Refs. 11, 16, and 23) relative to its value for the clean Cu(100) surface result in a small change in the positronium activation energy E_a with the alkali-metal coverage, in agreement with experiment.[11,16,23]

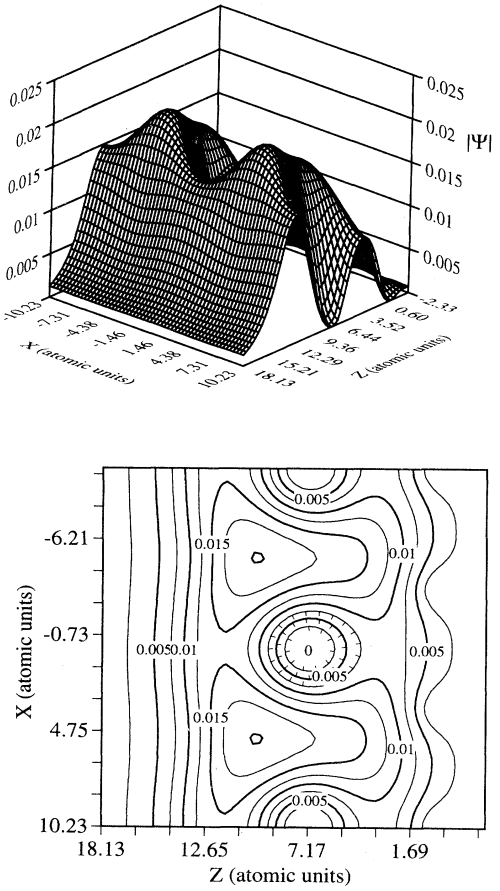

FIG. 10. Calculated ground-state wave function for a positron trapped in a surface state at a Cu(100) surface with an ordered hexagonal-close-packed arrangement of the Cs adsorbate. The upper panel shows the 3D plot. The lower panel shows the contour plot in the X-Z plane for $Y=0$. The vacuum is at the left in the lower panel. The minimum contour and the contour spacing are 0.0025 a.u.

III. ANNIHILATION CHARACTERISTICS

A. Positron annihilation with core-level electrons

Since core-level electrons are more tightly bound than valence electrons, electron-positron correlations are relatively less important in calculations of the positron-annihilation rate $\lambda_{n,l}$ with specific core-level electrons, described by n and l, than in calculations of the total annihilation rate λ (the inverse of the positron surface-state lifetime), which is dominated by annihilation with valence electrons.[37] We therefore expect the independent particle model (IPM),[37] which neglects electron-positron correlations, to provide a reasonable estimate of $\lambda_{n,l}$. Within the IPM,[37] the rate $\lambda_{n,l}$ is computed from the overlap of positron and electron densities:

$$\lambda_{n,l}=\pi r_0^2 c \int d^3r |\Psi_+(r)|^2 \left[\sum_i |\Psi^i_{n,l}(r)|^2 \right] , \quad (3)$$

where r_0 is the classical electron radius, c is the speed of light, Ψ^+ is the positron wave function, and $\Psi^i_{n,l}$ is the wave function of the core electron described by quantum numbers n and l. The summation is over all electron states in the atomic level defined by quantum numbers n and l. Comparison of experimental positron lifetimes with calculations of positron-annihilation rates in metals performed in Refs. 37–39 and angular correlation of annihilation radiation (ACAR) results,[40] indicate that it is necessary to multiply the IPM result by an enhancement factor (of the order of 1–3 for core electrons) to account approximately for the electron-positron correlation effects, which would tend to increase the positron-

annihilation rate. However, in those cases when one is interested only in relative changes of $\lambda_{n,l}$ as a function of adsorbate coverage, it is possible to neglect the enhancement of the positron-annihilation rate due to electron-positron correlations, since it is expected that the enhancement factor would not vary much with the atomic environment.[37–39]

B. Positron surface-state lifetime

The electron-positron correlation effects are much more significant for valence electrons as compared to core electrons. Therefore, in calculating the total annihilation rate λ of the surface-trapped positrons, we take correlation effects with valence electrons explicitly into account by using the local-density-approximation (LDA) approach,[33] within which λ (the inverse of the positron surface-state lifetime τ) is found from the following equation:

$$\lambda=\frac{\pi r_0^2 c}{e}\int d^3r\, n^+(r)n(r)\Gamma(n(r))\ , \tag{4}$$

where $n^+(\mathbf{r})$ is the positron charge density, $n(\mathbf{r})$ is the electron density, and $\Gamma(n(\mathbf{r}))$ is the annihilation enhancement factor in an electron gas of density $n(\mathbf{r})$, which takes account of the fact that the electrons are attracted toward the positively charged positron, thus increasing the overlap of the positron and core electron wave functions and hence the annihilation rate. In earlier calculations[41] the lifetime of a surface-trapped positron was computed over the entire distribution of the positron wave function. However, outside the metal surface the LDA must break down since the positron correlation potential is no longer related to the electron density at the position of the positron, but is due to the presence of a metal surface with a large number of accumulated electrons on it. Far from the surface the positron correlation potential must approach the long-range image potential. To correct for the inherent inconsistency with the modeling of the positron correlation potential, a cutoff point in the local contribution to the total annihilation rate within the LDA is introduced[42] as a point which divides space into the bulk and image-potential regions. The bulk and image-potential regions are defined as regions of space where the positron correlation potential is given by the LDA and image potentials, respectively. It is possible to modify the LDA result for λ by assuming the factor $\Gamma(n(\mathbf{r}))$ to be nonzero for all $\mathbf{r}$ inside the bulk region, and to be zero for all $\mathbf{r}$ inside the image-potential region, assuming the local annihilation rate in this region is zero. Recent many-body calculations within the bulk region for a homogeneous electron gas of various values of the electron-density parameter r_s result in the following interpolation form for the annihilation enhancement factor $\Gamma(n(\mathbf{r}))$:[33]

$$\Gamma(n(\mathbf{r}))=1+1.23r_s+0.8295r_s^{3/2}-1.26r_s^2 +0.3286r_s^{5/2}+r_s^3/6\ ,$$

where $(4\pi/3)r_s^3 n=1$.

C. Numerical results

We have calculated the total positron annihilation rate λ over the bulk region defined by the cutoff point. The core annihilation probabilities $p_{n,l}$ with the specific core electron shells, described by quantum numbers n and l, can be obtained by dividing the partial positron-annihilation rate $\lambda_{n,l}$ with the different core shells by the total positron-annihilation rate λ: $p_{n,l}=\lambda_{n,l}/\lambda$. The computed values of the positron surface-state lifetimes with cutoff τ and of the positron annihilation probabilities $p_{n,l}$ with Cu $3s$ and $3p$ and with Cs $4p$ and $4d$ core-level electrons for different ordered structures of the Cs adsorbate on the Cu(100) surface below and above the critical alkali-metal coverage are presented in Table I. It follows from our calculations that the shift in localization of the positron bound state from the Cs/Cu interface (at alkali-metal coverages below the critical coverage) to the vacuum side of the alkali-metal overlayer (at the Cs coverage of one physical monolayer) results in a sharp reduction of the magnitude of the overlap of the positron and the Cu $3s$ and $3p$ electron densities. Consequently, the sum of the probabilities for the positron trapped in the

TABLE I. Calculated values of positron surface-state lifetimes with cutoff, and of positron-annihilation probabilities with Cu $3s$ and $3p$ core-level electrons, as well as with Cs, $4p$ and $4d$ core-level electrons for clean and Cs-covered Cu(100) surfaces. All coverages are given in terms of the surface-atomic density of the hexagonal-close-packed array of Cs atoms on the Cu(100) surface, which corresponds to the Cs coverage of one physical monolayer [the maximum Cs coverage within a single layer on the Cu(100) surface].

System	Cs coverage (monolayer)	τ (ps)	Positron-annihilation probabilities with core-level electrons (%) Cu $3s$	Cu $3p$	Cs $4p$	Cs $4d$
Clean Cu(100)		615	0.915	3.348		
Cu(100)+Cs	0.124	509	0.602	2.202	0.024	0.079
Cu(100)+Cs	0.248	515	0.582	2.132	0.025	0.082
Cu(100)+Cs	0.496	543	0.457	1.672	0.038	0.127
Cu(100)+Cs	1.000	466	0.092	0.340	0.058	0.193

surface state to annihilate with Cu 3*s* and 3*p* core-level electrons at the alkali-metal coverage of one physical monolayer experiences a considerable drop to 0.43% compared with 4.26% for the clean Cu(100) surface, and compared with 2.80%, 2.71%, and 2.13% for the cases of the ordered $p(4\times4)$, $c(4\times4)$, and $p(2\times2)$ structures of the Cs adsorbate on the Cu(100) surface, respectively, which correspond to alkali-metal coverages below the critical Cs coverage. It also follows from our calculations that at Cs coverages below the critical alkali-metal coverage the sum of the positron-annihilation probabilities with Cu 3*s* and 3*p* core-level electrons, σ_{Cu}, considerably exceeds the sum of the positron-annihilation probabilities with Cs 4*p* and 4*d* core-level electrons, σ_{Cs}. At the alkali-metal coverage of one physical monolayer, $\sigma_{Cu}\approx\sigma_{Cs}$, and both are considerably smaller than the clean Cu(100) surface value of σ_{Cu}. The change in calculated positron surface-state lifetimes with the Cs coverage reflects the change in the location of the maximum of the positron surface state for different alkali-metal coverages as well as the change in the spatial extent of the bulk region and of the positron surface state with the Cs coverage.

IV. DISCUSSION

The theoretical results presented in this paper for the localization of the positron surface state and for annihilation probabilities of surface-trapped positrons with relevant Cu core-level electrons are consistent with the predictions of Nieminen and Jensen[25] and calculations performed in Ref. 11 only for Cs coverages below the critical alkali-metal coverage of approximately 0.7 physical monolayer. At these Cs coverages the calculated positron wave function is found to have its maximum between the Cs overlayer and the Cu substrate. The fact that the calculated positron wave function is not pushed away from the Cu substrate by the alkali-metal overlayer leads to the prediction that the annihilation probabilities of surface-trapped positrons with relevant Cu core-level electrons at these alkali-metal coverages do not vary substantially with Cs coverage. However, our calculations indicate that the positron surface state is found to be localized mainly on the vacuum side of the alkali-metal overlayer at the Cs coverage of one physical monolayer. This location of a positron bound state results in a dramatic decrease of the annihilation probabilities of a surface-trapped positron with relevant Cu core-level electrons, since the overlap between the positron wave function and the Cu 3*s* and 3*p* core-level electron functions considerably decreases at this coverage. These theoretical results deviate significantly from predictions of Nieminen and Jensen[25] and calculations performed in Ref. 11. In calculations of positron surface states for alkali-metal-covered transition-metal surface performed in Refs. 11 and 25, the authors neglected the fact that the alkali-metal overlayer on the transition-metal surface at coverages close to one physical monolayer can be considered as a metallic adsorbate,[5–8] and the correlation effects in Cs/Cu(100) at these coverages should be treated differently than in the case of the Cs coverage below the critical one of approximately 0.7 physical monolayer.

First-principles calculations of the positron surface state at the (100) surface of Cu covered with submonolayers of Cs performed in this paper provide theoretical justifications for the phenomenological double-well model used in Refs. 15 and 16 to explain the sharp drop in the normalized Cu $M_{2,3}VV$ PAES intensity at the critical Cs coverage.

In Fig. 11 we compare our calculations of the sum of the annihilation probabilities of a positron trapped in the surface state with Cu 3*s* and 3*p* core-level electrons for different ordered arrangements of the Cs adsorbate normalized to the clean Cu(100) surface value with the results of measurements performed at 163 K of the normalized Cu $M_{2,3}VV$ PAES intensity, I_P, as a function of the ratio R of the electron-annihilation-induced Cs (563 eV) to the Cu (920 eV) Auger peaks for the system Cs/Cu(100) taken from Ref. 11. The Cs coverage is approximately proportional to the Auger ratio R. A ratio of 0.14 corresponds to the alkali-metal coverage of one physical monolayer. Since core-hole excitations in the outer-shell core levels result in an Auger-electron emission[24] with almost unit probability, the intensity of the positron-annihilation-induced Cu $M_{2,3}VV$ Auger signal normalized to the clean Cu(100) surface value and to the fraction of positrons that annihilate in the surface state should be approximately proportional to the sum of the positron-annihilation probabilities with Cu 3*s* and 3*p* core-level electrons (contributions to the PAES intensity from deeper core levels are much smaller due to the repulsion of the positron from the nucleus).[14] The propor-

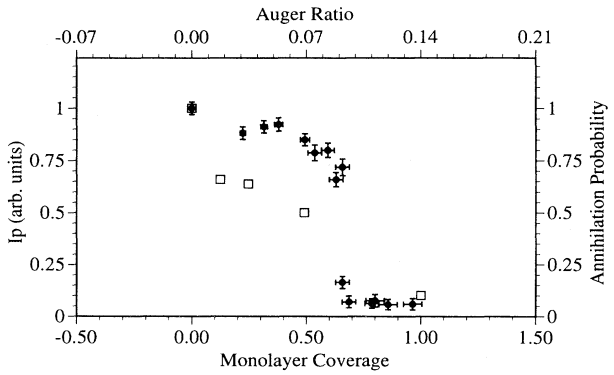

FIG. 11. Calculated sum of the annihilation probabilities (open squares) of a positron trapped in surface states with Cu 3*s* and 3*p* core-level electrons for various ordered arrangements of the Cs adsorbate on the Cu(100) surface normalized to the clean Cu(100) surface value. Measured values of the intensity of the positron-annihilation-induced Cu $M_{2,3}VV$ Auger signal, normalized to the clean Cu(100) surface value and to the fraction of positrons that annihilate in the surface state, I_P (closed circles), as a function of the ratio of the electron-annihilation-induced Cs (563 eV) to the Cu (920 eV) Auger peaks for the system Cs/Cu(100) at 163 K are taken from Ref. 11. The Cs coverage is approximately proportional to the Auger ratio. A ratio of 0.14 corresponds to the alkali-metal coverage of one physical monolayer.

tionality is not exact because of the attenuation caused by the inelastic scattering of the outgoing Auger electrons exiting from the surface as they traverse the Cs overlayer. Thus the increased attenuation resulting from the increased Cs coverage would cause the measured PAES intensity to fall off slightly faster with the Cs coverage than the core-annihilation probability. We estimate that this effect would lead to a deviation of less than 20% from proportionality over the range in which the Cu Auger signal is significant.[11,15,16] As can be seen from Fig. 11, the alkali-metal coverage dependence of the calculated sum of annihilation probabilities of a positron trapped in a surface state with Cu 3*s* and 3*p* core-level electrons reproduces changes with the Cs coverage of the normalized Cu $M_{2,3}VV$ PAES intensity. At low Cs coverages both the sum of the Cu 3*s* and 3*p* core-annihilation probabilities and the measured Cu $M_{2,3}VV$ PAES intensity are a substantial fraction of the values obtained from the clean Cu(100) surface. At the Cs coverage corresponding to one physical monolayer both the calculated and measured values are only a few percent of the clean Cu surface values. This sharp decrease seen in the normalized Cu $M_{2,3}VV$ PAES intensity at an alkali-metal coverage of approximately 0.7 physical monolayer can be understood in terms of the structural phase transition in the Cs overlayer at that coverage from a disordered distribution of adatoms to an arrangement of adsorbate metallic islands with a locally ordered hexagonal-close-packed structure, as indicated in molecular-dynamics calculations.[15,16,34] It should be noted that at low coverages the Cs overlayer is not fully ordered. Consequently, calculations performed for the ordered Cs overlayers on the Cu(100) surface for alkali-metal coverages below the critical Cs coverage probably underestimate annihilation probabilities of the surface-trapped positrons with Cu 3*p* core-level electrons due to the fact that in a disordered system the positron can be expected to seek out regions of lower Cs coverage and, thus, to be in a closer contact with the Cu core.

At the present time, the available experimental data for Cs PAES intensities do not permit a comparison of theory and experiment corresponding to the one shown in Fig. 11 for Cu. As discussed in Sec. III, our calculations indicate that even at high-Cs coverages the sum of probabilities of a positron trapped in a surface state to annihilate with Cs 4*p* and 4*d* core-level electrons is only a small fraction of the sum of positron-annihilation probabilities with Cu 3*s* and 3*p* core-level electrons for the clean Cu(100) surface. In addition, at high-Cs coverages, even when the temperature is lowered to inhibit the thermal desorption, a minimum of approximately 70% of the incident positrons are emitted as positronium, making them unavailable to contribute to the PAES signal [as compared with approximately 50% of the positronium emission for the clean Cu(100) surface at room temperature]. As a consequence, the Cs $N_{4,5}VV$ PAES signal can be expected to be only a small fraction of the Cu $M_{2,3}VV$ PAES signal for the clean Cu(100) surface, thus making it very difficult to measure using currently available positron beam fluxes and reasonable data accumulation times. Preliminary measurements[34] performed at 173 K indicate that, at the Cs coverage corresponding to approximately one physical monolayer, the relative Cs $N_{4,5}VV$ PAES intensity [normalized to the Cu $M_{2,3}VV$ PAES intensity from the clean Cu(100) surface and to the fraction of positrons that annihilate in the surface state] is 0.07 ± 0.06. The Cu $M_{2,3}VV$ PAES intensity at this Cs coverage was found to be equal, within the accuracy of the measurement, to the Cs $N_{4,5}VV$ PAES intensity. These values may be compared with the sum of the annihilation probabilities of the positron trapped in the surface state with relevant Cu and Cs core-level electrons calculated for the Cs coverage of one physical monolayer divided by the sum of the Cu 3*s* and 3*p* core-annihilation probabilities for the clean Cu(100) surface (see Table I): 0.06 for the Cs 4*p* and 4*d* core-level electrons, and 0.10 for the Cu 3*s* and 3*p* core-level electrons, respectively. Thus the results of preliminary low-temperature measurements of the Cu and Cs PAES intensities are consistent with theoretical predictions.

V. CONCLUSIONS

We have performed a microscopic analysis of the alkali-metal coverage dependence of the normalized Cu $M_{2,3}VV$ PAES intensity by performing first-principles calculations of the positron surface states and corresponding positron-annihilation characteristics for the Cu(100) surface covered with submonolayers of Cs. The positron has been treated as a single charged particle trapped in a correlation well in the proximity of surface atoms. Image-potential-induced positron surface states have been calculated for various ordered structures of the Cs adsorbate on the Cu(100) surface below and above the critical alkali-metal coverage of 0.7 physical monolayer using the corrugated-mirror model in a full three-dimensional geometry.

The positron surface state has been found to be localized mainly in the region of the Cs/Cu(100) interface at Cs coverages below the critical alkali-metal coverage. Contrary to previous calculations of the positron surface state at the alkali-transition-metal surface, we have taken into consideration explicitly that the Cs overlayer at coverages close to one physical monolayer behaves as a metallic adsorbate. At the Cs coverage corresponding to one physical monolayer the positron surface state has been found to be mainly localized on the vacuum side of the Cs adsorbate. It has been found that the Cs adsorption on the Cu(100) surface leads to an increase in the positron surface-state binding energy. This increase in the positron binding energy together with the decrease of the electron work function for Cs/Cu(100) relative to its value for the clean Cu(100) surface result in a small change in the positronium activation energy with alkali-metal coverage, in agreement with experiment.

The impact of various arrangements of the Cs adsorbate on annihilation probabilities of surface-trapped positrons with Cu 3*s* and 3*p* core-level electrons as well as with Cs 4*p* and 4*d* core-level electrons has been studied, and positron surface-state lifetimes have been calculated. It has been shown that due to the location of the positron surface state mainly between the Cs adsorbate and the Cu(100) surface below the critical alkali-metal coverage,

the sum of the annihilation probabilities of surface-trapped positrons with Cu 3*s* and 3*p* core-level electrons does not change significantly from the clean Cu surface value. The shift in localization of the positron surface state from the Cs/Cu interface to the vacuum side of the Cs overlayer due to the metallization of the Cs adsorbate has resulted in a sharp decrease in the calculated combined positron-annihilation probabilities with Cu 3*s* and 3*p* core-level electrons.

Trends found in the calculations of annihilation probabilities of positrons trapped in surface states for various ordered structures of the Cs adsorbate on the Cu(100) surface are in agreement with experimental measurements of the positron-annihilation-induced Cu $M_{2,3}VV$ Auger signal with the Cs coverage below and above the critical alkali-metal coverage of approximately 0.70 physical monolayer, performed at 163 K. In particular, they reproduce the sharp reduction in the Cu PAES intensity observed at a Cs coverage of one physical monolayer. The results of the calculations of positron-annihilation probabilities with the Cs 4*p* and 4*d* core-level electrons are consistent with measurements of a small low-temperature Cs $N_{4,5}VV$ PAES signal for the alkali-metal coverage of one physical monolayer on the Cu(100) surface. Thus the results of PAES studies of the Cu(100) surface covered with submonolayers of Cs are consistent with the image-potential-induced surface-state model.

ACKNOWLEDGMENTS

We would like to thank A. P. Mills, Jr., K. G. Lynn, R. M. Nieminen, P. Hautojärvi, and K. O. Jensen for useful and stimulating discussions. This work was supported by the National Science Foundation, the Texas Advanced Research Program, the Robert A. Welch Foundation, and the Texas Advanced Technology Program.

*Permanent address: Department of Physics, Kazan State University, Kazan 420008, Russia.

[1]J. P. Muscat and D. M. Newns, Prog. Surf. Sci. **9**, 1 (1978); Surf. Sci. **84**, 262 (1979).

[2]N. D. Lang, Phys. Rev. B **4**, 4234 (1971).

[3]E. Wimmer, A. J. Freeman, M. Weinert, H. Krakauer, J. R. Hiskes, and A. M. Karo, Phys. Rev. Lett. **48**, 1128 (1982); M. Posternak, H. Krakauer, A. J. Freeman, and D. D. Koelling, Phys. Rev. B **21**, 5601 (1980); E. Wimmer, A. J. Freeman, J. R. Hiskes, and A. M. Karo, *ibid.* **28**, 3074 (1983); P. Soukiassian, R. Riwan, J. Lecante, E. Wimmer, S. R. Chubb, and A. J. Freeman, *ibid.* **31**, 4911 (1985).

[4]Wang Ning, Chen Kailai, and Wang Dingsheng, Phys. Rev. Lett. **56**, 2759 (1986).

[5]H. Ishida and K. Terakura, Phys. Rev. B **36**, 4510 (1987); **38**, 5752 (1988).

[6]S. A. Lindgren and L. Wallden, Phys. Rev. B **22**, 5967 (1980).

[7]R. L. Gerlach and T. N. Rhodin, Surf. Sci. **17**, 32 (1969).

[8]D. M. Riffe, G. K. Wertheim, and P. H. Citrin, Phys. Rev. Lett. **64**, 571 (1990); G. K. Wertheim, D. M. Riffe, and P. H. Citrin, Phys. Rev. B **49**, 4834 (1994); A. B. Andrews, D. M. Riffe, and P. H. Citrin, *ibid.* **49**, 8396 (1994).

[9]C. A. Papageorgopoulos, Phys. Rev. B **25**, 3740 (1982).

[10]J. Cousty, R. Riwan, and P. Soukiassian, Surf. Sci. **152/153**, 297 (1985).

[11]A. R. Koymen, K. H. Lee, D. Mehl, Alex Weiss, and K. O. Jensen, Phys. Rev. Lett. **68**, 2378 (1992).

[12]D. Mehl, A. R. Koymen, Kjeld O. Jensen, Fred Gotwald, and Alex Weiss, Phys. Rev. B **41**, 799 (1990).

[13]N. G. Fazleev, J. L. Fry, K. Kuttler, G. Yang, and A. H. Weiss, Bull. Am. Phys. Soc. **39**, 81 (1994).

[14]Kjield O. Jensen and A. Weiss, Phys. Rev. B **41**, 3928 (1990).

[15]N. G. Fazleev, J. L. Fry, J. H. Kaiser, A. R. Koymen, T. D. Niedzwiecki, and Alex Weiss, in *Positron Beams for Solids and Surfaces,* edited by E. Ottewitte and A. Weiss, AIP Conf. Proc. No. **303**, 208 (AIP, New York, 1994); J. L. Fry, N. G. Fazleev, A. Weiss, A. R. Koymen, J. H. Kaiser, K. Kuttler, and T. D. Niedzwiecki, Bull. Am. Phys. Soc. **38**, 800 (1993).

[16]N. G. Fazleev, J. L. Fry, J. H. Kaiser, A. R. Koymen, K. H. Lee, T. D. Niedzwiecki, and A. Weiss, Phys. Rev. B **49**, 10 577 (1994).

[17]Alex Weiss, R. Mayer, M. Jibaly, C. Lei, D. Mehl, and K. G. Lynn, Phys. Rev. Lett. **61**, 2245 (1988); Alex Weiss, Mohammed Jibaly, Chun Lei, David Mehl, Rulon Mayer, and K. G. Lynn, in *Proceedings of the Eighth International Conference of Positron Annihilation, 1988,* edited by L. Dorikens-Vanpraet, M. Dorikens, and D. Segers (World Scientific, Singapore, 1989); A. Weiss, Mater. Forum **105-110**, 511 (1992); Solid State Phenom. **28 & 29**, 317 (1992).

[18]A. Joshi, L. E. Davis, and P. W. Palmberg, in *Methods of Surface Analysis,* edited by A. W. Czanderna (Elsevier, Amsterdam, 1975).

[19]C. H. Hodges and M. J. Stott, Solid State Commun. **12**, 1153 (1973); A. P. Mills, Jr., *ibid.* **31**, 623 (1979); K. G. Lynn, Phys. Rev. Lett. **43**, 391 (1979); K. G. Lynn and D. O. Welch, Phys. Rev. B **22**, 99 (1980); I. J. Rosenberg, A. H. Weiss, and K. F. Canter, J. Vac. Sci. Technol. **17**, 253 (1980).

[20]R. Mayer, A. Schwab, and A. Weiss, Phys. Rev. B **42**, 1881 (1990).

[21]K. H. Lee, A. R. Koymen, D. Mehl, K. O. Jensen, and A. Weiss, Surf. Sci. **264**, 127 (1992).

[22]A. R. Koymen, K. H. Lee, G. Yang, K. O. Jensen, and A. H. Weiss, Phys. Rev. B **48**, 2020 (1993).

[23]D. W. Gidley, A. R. Koymen, and T. W. Capehart, Phys. Rev. B **37**, 2565 (1988); P. M. Platzman and N. Tzoar, *ibid.* **33**, 5900 (1986); P. J. Schultz and K. G. Lynn, Rev. Mod. Phys. **60**, 701 (1988), and references therein.

[24]E. J. McGuire, Phys. Rev. A **3**, 587 (1971); **5**, 1052 (1972).

[25]R. M. Nieminen and Kjield O. Jensen, Phys. Rev. B **38**, 5764 (1988).

[26]R. M. Nieminen and M. J. Puska, Phys. Rev. Lett. **50**, 281 (1983).

[27]O. Gunnarsson and B. I. Lundqvist, Phys. Rev. B **13**, 4276 (1976).

[28]D. M. Ceperly and B. J. Adler, Phys. Rev. Lett. **45**, 566 (1980).

[29]N. W. Ascroft and N. D. Mermin, *Solid State Physics* (Holt, Rinehart, and Winston, New York, 1976).

[30]M. Weinert and R. E. Watson, Phys. Rev. B **29**, 3001 (1984).

[31]F. Herman and S. Skillman, *Atomic Structure Calculations* (Prentice-Hall, Englewood Cliffs, NJ, 1963).

[32]J. Arponen and E. Pajanne, Ann. Phys. (N.Y.) **121**, 343 (1979).
[33]E. Boronski and R. M. Nieminen, Phys. Rev. B **34**, 3820 (1986).
[34]N. G. Fazleev, J. L. Fry, K. Kuttler, A. R. Koymen, and A. H. Weiss, Appl. Surf. Sci. **85**, 26 (1995).
[35]S. Andersson and B. Kasemo, Surf. Sci. **32**, 78 (1972).
[36]N. D. Lang and W. Kohn, Phys. Rev. B **7**, 3541 (1973).
[37]E. Bonderup, J. U. Andersen, and D. N. Lowy, Phys. Rev. B **20**, 883 (1979).
[38]K. O. Jensen, J. Phys. Condens. Matter **1**, 10 595 (1989).
[39]B. Chakraborty, in *Positron Annihilation,* edited by P. C. Coleman, S. C. Sharma, and L. M. Diana (North-Holland, Amsterdam, 1982), p. 207.
[40]M. Sob, Solid State Commun. **53**, 255 (1985).
[41]M. J. Puska and R. M. Nieminen, J. Phys. F **13**, 333 (1983); J. E. Inglesfield and M. J. Stott, *ibid.* **10**, 253 (1980); R. M. Nieminin and M. Manninen, Solid State Commun. **15**, 403 (1974).
[42]R. M. Nieminen, M. J. Puska, and M. Manninen, Phys. Rev. Lett. **63**, 1298 (1984).